

CHAPTER 13

THE FIFTH COMING OF VORTICES

In 1993 I discovered a unique spacetime spiral element called the *toryx*. The ability of the toryx to be turned inside out made it perfect for modeling polarized prime elements of matter. At about the same time I discovered a close offspring of the toryx called the *helyx* that appeared to be ideal for modeling polarized prime elements of radiation particles. These two discoveries led me to the development of a new version of the vortex theory called *Three-Dimensional Spiral String Theory* (3D-SST).

As any new theory, 3D-SST includes several ideas that some scientists may find controversial. To avoid any confusion, the author separated the parts of the theory that are based on prudent conventional assumptions from the parts that required some speculative propositions. Following this approach, Chapter 13 describes a stand-alone spacetime model of toryx and helyx. The model is based on several clear non-speculative assumptions, and its equations can readily be verified by using commonly known mathematical methods. Chapters 14 and 15 outline some possible applications of the spacetime model for defining main properties of prime elements of the universe and their offspring, the particles of ordinary matter described by the conventional physics, and also the exotic particles of dark matter and dark energy.

Chapter 16 outlines a possible way of unification of strong, superstrong (color), gravitational, and electric forces. Here again the proposed theory is divided in two parts. The first part describes in pure mathematical non-speculative terms the Coulomb forces between thin rings with evenly distributed electric charges. Then the second part utilizes the above mathematical model to explain strong, superstrong (color) and gravitational forces between particles.

THE UNIVERSAL HELICOLA

In 1992, I knew nothing about the existence of the vortex theory. It all started in December of that year during a dinner conversation with my son Gene, who was finishing his last year of high school. Although, besides high school, I studied physics thoroughly while doing both M.S. and Ph.D degrees, none of my professors had ever mentioned this theory,

and I did not remember any references to this subject in the textbooks available to me. For some reason Gene was briefly in a philosophical mood during that fateful evening, and while looking at a crumb of bread, he made a casual observation: “There is probably another world inside that piece.”

Even though I heard this notion more than once before, somehow it registered in my mind differently this time. So, I tend to agree with Gene and with all the other people who believe that there is a world that looks like a small pinhead to us and also that our world may look like a pinhead to beings of a much larger world than ours. It was, however, one thing to agree with the exciting idea of a multiple-level universe and a completely different thing to envision it. Intuitively, I thought that the solution of this problem could be found in geometry. It turned out to be a right direction for my search. After a few sleepless nights and almost uninterrupted thinking during a vacation with my wife at a beautiful resort in Phoenix, Arizona, I discovered a geometrical shape that would perfectly represent the infinitude of the world and its repetitious character in both enlarging and diminishing directions. This shape was the endless multiple-level spiral that I named *helicola*. Impressed by its beauty and simplicity along with its unique properties, I became convinced that *helicola* certainly deserves to be called the “spiral of the spirals.”

But is the *helicola* merely a product of my abstract imagination? A few days later, after looking at beautiful blue Arizona sky, I realized that *helicola* was present in nature since the beginning of times. Moreover, it must be at the core of the universe. You may rightfully be puzzled by my discovery. The astronomers have been scanning the skies for many centuries. The Hubble Telescope had recently provided us with spectacular views of previously unseen galaxies and with unimaginable extraterrestrial formations located many billion light years away from us. But, besides confirming the already known fact that many galaxies are spiral, nobody had found yet any presence of spiral shape in other celestial structures. Is it really there? Of course, it is.

There is a simple explanation why, in spite of a great resolution of contemporary telescopes, we failed to detect the spiral nature of the universe in the instant images of visible matter:

The hidden spiral nature of the universe will immediately become visible as soon as we begin looking not at the matter, but at the way it moves in space.

Please join me in the exciting venture of discovering the spiral nature of the universe. In the course of this venture, we are not going to use any telescopes; neither will we use a yoga technique employed by Leadbeater

and Besant. Instead, we will utilize available astronomical data assisted by our common sense. Let us begin from asking a simple question: “What is the path of the Earth in space?” Most people whom I asked this question had promptly responded that this path is *elliptical*. Some of them even referred to the Kepler’s Laws to support their answer. Well, although many students may still get an A in school for giving this answer, but, as you will see in a moment, this answer does not describe a true trajectory of our planet. Unfortunately, many of our teachers failed to mention to us the fact that Kepler derived his laws when the Sun was believed to be a center of the universe. It was a revolutionary idea during his times, but certainly not now when we know that the Sun is merely one of the stars moving around the center of our galaxy, Milky Way, and that our galaxy is also moving in space.

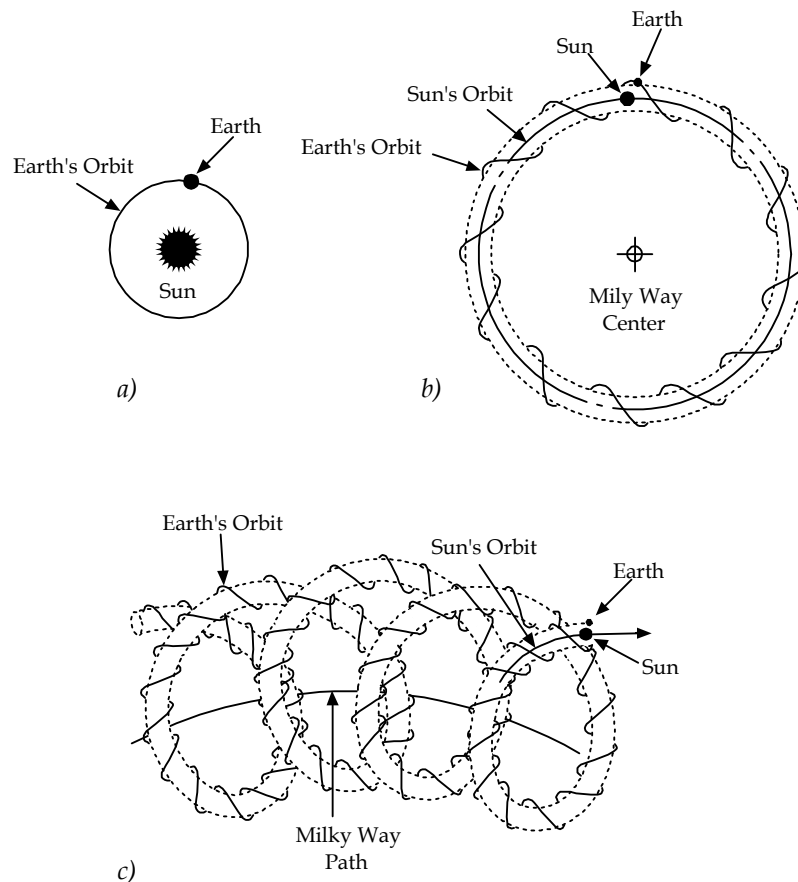


Fig. 13.1. Appearances of the Earth’s path in space.

Thus, the appearance of the Earth's path in space depends on a position of an observer. The observer located above the center of the Sun will see the Earth moving along its elliptical path around the Sun (Fig. 13.1a) at average velocity of 29.79 km/s, exactly as we were taught in school. However, the appearance of the Earth's trajectory will immediately change as soon as the observer relocates to a place distant from the Sun. Since the Sun moves around the center of our galaxy, the Milky Way, at average velocity of about 240 km/s, the observer located above the center of our galaxy will see the Earth's path as a helical spiral wound around the Sun's path (Fig. 13.1b).

Is this a final "world line" for our planet? No, it is not. According to the latest astronomical data, our galaxy rushes towards the constellation Hydra at velocity of 600 km/s. So, to an observer located far away from the path of the Milky Way, the Earth's path will look like a dual-level spiral in which one helical spiral is wound around another helical spiral (Fig. 13.1c). Nowadays we know nothing about a gigantic mysterious object around which the Milky Way moves. But an observer located far away from the gigantic mysterious object would see the Earth's path as a triple-level helical spiral. To the observer located at even greater distance from the Earth, the "world line" of our planet will look as a quadruple-level helical spiral, and so on and so on. This multiple-level helical spiral is *helicola*. Thus,

Helicola is a multiple-level spiral in which a helical spiral of a certain level is wound around a spiral path of a helical spiral of an adjacent lower level.

We are not just passive observers of *helicola*, but its intimate companions. All of us are moving continuously along its multiple levels. The precise "world line" of each person depends on his or her location. For instance, those of us who are located at the altitude of New York will advance every one hour about 1200 km along the level n of *helicola* that coincides with the trajectory of the rotation of the Earth's surface around its axis. During the same time, we will advance about 107,240 km along the level $(n - 1)$ of *helicola* that coincides with the orbital path of the Earth around the Sun. In addition, during the same one hour we will advance about 864,000 km along the level $(n - 2)$ of *helicola* that is the orbital path of the Sun around the center of galaxy. The next level $(n - 3)$ of *helicola* coincides with the trajectory of the center of our galaxy in its journey towards the constellation Hydra. This motion will add another whooping 2,160,000 km to our travel distance covered during the same one hour. But, the constellation Hydra is not standing still either. So, during the same hour, we may have also advanced many millions of

kilometers along the level $(n - 4)$ of helicola, also along the levels $(n - 5)$, $(n - 6)$, and so on and so on.

Our path in space is certainly different from the one impressed in our minds from learning about Kepler's elliptical orbits and the galaxies flying apart after the Big Bang. To the delight of some scholars who avoid discussing new ideas that are not widely accepted by the scientific community, the discovery of helicola required neither a help from any speculative propositions nor a use of any unproven astronomical data. All the facts were available long ago, and I was able to discover the celestial helicola only by looking at the same data from a different angle.

Soon after our return back home from Phoenix, in 1993, I wrote a short essay "Multiple-Level Universe" and sent a few copies to several scientists in the United States. Among the received responses the most encouraging was from Dr. Carlo Rovelli of the University of Pittsburgh who described my little essay as "delightful and stimulating." This marked a beginning of my serious research on spirals that still continues without any interruption. One of the first questions that bothered me the most was: "What is the origin of the spiral motion in the universe?" The more I read about the vortex theory the more I tended to agree with some developers of this theory that the origin of the spiral motion in the universe is hidden in the dynamics of its internal structure that goes all the way down to the *prime elements of matter and energy*.

CONSTRUCTION OF TORYX

I began my research on spirals from finding an abstract mathematical model for a simplest version of helicola. I chose a geometrical shape that had only two levels of helicola, the minimum number of levels for the spiral to be qualified as helicola. You can easily follow the construction of this shape. Consider two points, m and n in Figures 12.2 and 12.3. Both points are separated from one another by 180 degrees and rotate around a pivot point O at rotational velocity V_{1r} . These points create two circular traces A_1 with radius r_1 called the *toryx leading string*.

As shown in Figures 12.2 and 12.3, the points m and n serve as pivot points for the points a and b separated from one another by 180 degrees and moving along a circle with radius r_2 . Rotational velocities of the points a are indicated as V_{2r} . The overall motions of the points m , n , a , and b create two sets of double-toroidal spiral traces A_2 separated from one another by 180 degrees. One set is associated with the pivot point m , while the other one with the pivot point n . The two sets of the double-toroidal spiral traces form the *toryx trailing string* A_2 . The radius of the toryx eye r_i is called the *inversion radius of trailing string*. Physical meaning of this name will be clear later.

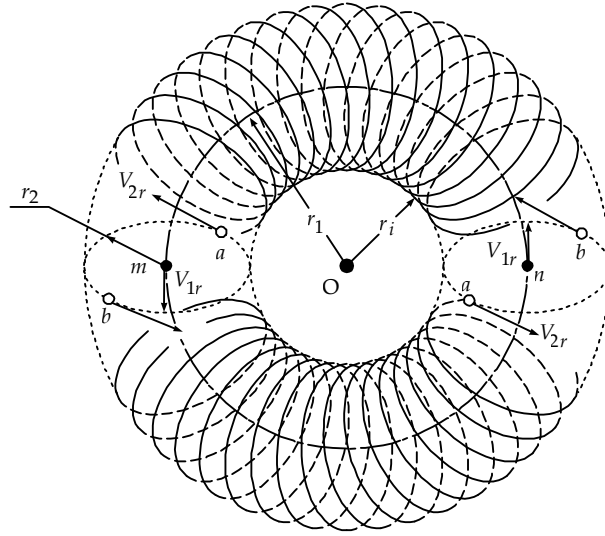


Figure 12.2. Construction of toryx.

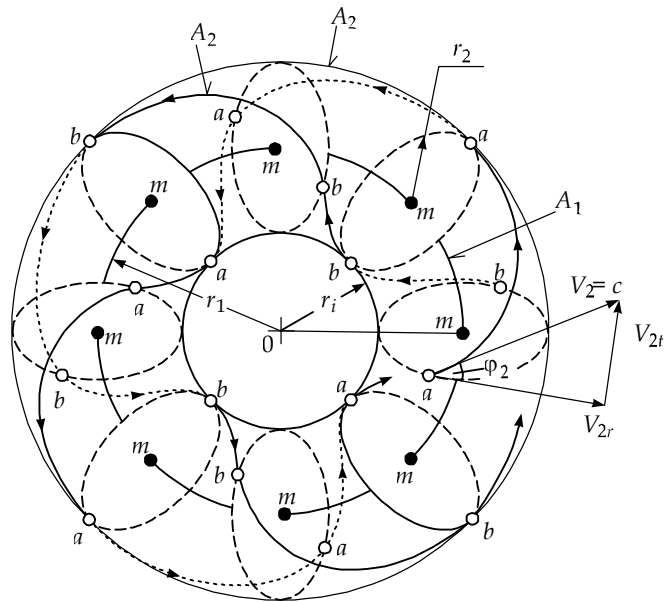


Figure 12.3. Construction of one of two double-toroidal trailing strings.

One of the most important features of the toryx is a capability of its double toroidal trailing string to propagate along its spiral path in

synchrony with the double-circular leading string. The requirement for the synchronization of motions of these strings is met when rotational velocity of leading string V_{1r} is equal to translational velocity of trailing string V_{2t} ($V_{1r} = V_{2t}$). According to the Pythagorean Theorem for the right triangle, spiral velocity of trailing string V_2 is equal to a geometrical sum of rotational and translational velocities of this string, V_{2r} and V_{2t} (Fig. 13.4).

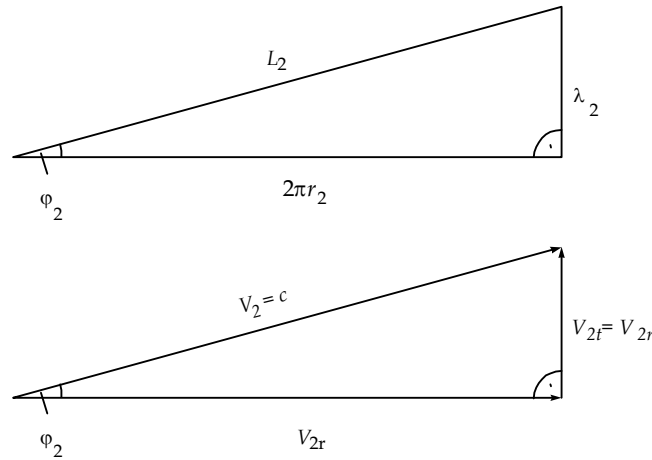


Figure 13.4. Spacetime parameters of toryx.

Besides the already mentioned parameters, the spacetime properties of toryx can also be described by several other parameters of leading and trailing strings, including the lengths of one winding of the strings L_1 and L_2 , string wavelengths λ_1 and λ_2 , string frequencies f_1 and f_2 , time periods T_1 and T_2 , the number of windings w_1 and w_2 , and steepness angles φ_1 and φ_2 . Because leading string is circular, $\lambda_1 = 0$, $w_1 = 1$, and $\varphi_1 = 0$.

SPACETIME PARAMETERS OF TORYX

Let us begin our story from describing the fundamental spacetime equations for the toryx. The purpose of these equations is two-fold. Firstly, they drastically reduce a variety of possible spacetime configurations of toryces, and secondly, they yield the spacetime properties of the toryx that could readily be associated with physical properties of potential prime elements of nature. The fundamental equations shown in Table 13.1 establish the assumed relationships between the spacetime properties of leading and trailing strings of toryx.

To a delight of the lovers of a simple math, the fundamental spacetime equations of toryx use only basic mathematical functions: addition, subtraction, multiplication, division, and trigonometry. The meaning of these equations is very clear. Equation (13-1) states that the difference between the radii of leading and trailing strings r_1 and r_2 is equal to the inversion radius of trailing string r_i that is constant. Equation (13-2a) requires the length of one winding of trailing string L_2 to be equal of that of leading string L_1 . Equation (13-2b) stipulates that, for the middle of trailing string, the cosine of steepness angle of this string φ_2 is equal to the ratio of radii of trailing and leading strings r_2 and r_1 . It shall be noted that Equations (13-2a) and (13-2b) yield the same spacetime toryx characteristics, and can be used interchangeably.

Table 13.1. Fundamental spacetime equations for toryx.

Parameter	Equation	Range
Inversion radius of trailing string	$r_i = r_1 - r_2 = \text{const.}$ (13-1)	$-\infty < r_1 < +\infty$ $-\infty < r_2 < +\infty$
Length of one winding of trailing string	$L_2 = L_1$ (13-2a)	$-\infty < L_1 < +\infty$
Steepness angle of trailing string	$\cos\varphi_2 = \frac{r_2}{r_1}$ (13-2b)	$-\infty < \cos\varphi_2 < +\infty$
Spiral velocity of trailing string.	$V_2 = \sqrt{V_{2t}^2 + V_{2r}^2} = c$ (13-3)	$-\infty < V_{2t}^2 < +\infty$ $-\infty < V_{2r}^2 < +\infty$

You may readily recognize in Equation (13-3) a particular case of the Pythagorean Theorem for the right triangle. In application to the toryx this theorem states that spiral velocity of trailing string V_2 is equal to the geometrical sum of translational and rotational velocities of trailing string V_{2t} and V_{2r} . Since $V_{2t} = V_{1r}$, spiral velocity of trailing string V_2 is also equal to the geometrical sum of rotational velocities of leading and trailing strings V_{1r} and V_{2r} . In addition, according to Equation (13-3), spiral velocity of trailing string V_2 is constant and equal to the so-called *ultimate string velocity* c .

So far, everything is very simple and easy to understand. But, we shall recognize a very important fact that to maintain spiral velocity of trailing string constant while it propagates along its spiral path, the rotational and translational components of the spiral velocity must vary. Also must vary are steepness angle and wavelength of trailing string. Consequently, in spite of their simplicity, the three fundamental equations of toryx yield very sophisticated and, at the same time, unique

spacetime properties of the toryx described in the remaining sections of this chapter.

Table 13.2. Equations for the spacetime properties of toryx.

Parameters	Leading string	Trailing string
Relative string radius	$b_1 = \frac{r_1}{r_i}$	$b_2 = \frac{r_2}{r_i} = b_1 - 1$
Steepness angle	$\varphi_1 = 0$	$\cos \varphi_2 = \frac{b_1 - 1}{b_1}$
Relative wavelength	$\eta_1 = \frac{\lambda_1}{2\pi r_i} = 0$	$\eta_2 = \frac{\lambda_2}{2\pi r_i} = \sqrt{2b_1 - 1}$
Relative length of one string winding	$l_1 = \frac{L_1}{2\pi r_i} = b_1$	$l_2 = \frac{L_2}{2\pi r_i} = b_1$
The number of windings per string	$w_1 = 1$	$w_2 = \frac{b_1}{\sqrt{2b_1 - 1}}$
Relative translational velocity	$\beta_{1t} = \frac{V_{1t}}{c} = 0$	$\beta_{2t} = \frac{V_{2t}}{c} = \frac{\sqrt{2b_1 - 1}}{b_1}$
Relative rotational velocity	$\beta_{1r} = \frac{V_{1r}}{c} = \frac{\sqrt{2b_1 - 1}}{b_1}$	$\beta_{2r} = \frac{V_{2r}}{c} = \frac{b_1 - 1}{b_1}$
Relative spiral velocity	$\beta_1 = \frac{V_1}{c} = \frac{\sqrt{2b_1 - 1}}{b_1}$	$\beta_2 = \frac{V_2}{c} = 1$
Relative frequency	$\delta_1 = \frac{f_1}{f_i} = \frac{\sqrt{2b_1 - 1}}{b_1^2}$	$\delta_2 = \frac{f_2}{f_i} = \frac{1}{b_1}$
Relative time period	$t_1 = T_1 f_i = \frac{b_1^2}{\sqrt{2b_1 - 1}}$	$t_2 = T_2 f_i = b_1$

At this time, we will only expose some hidden intricacies of four deceptively simple fundamental spacetime equations of toryx:

- Unlike a general view that the radii of a toroidal spiral must be only positive, the radii of both leading string r_1 and trailing string r_2 of the toryx can be either positive or negative, but their difference remains equal to a constant positive value of inversion radius of trailing string r_i according to Equation (13-1).

- Unlike a general view that the range of cosine of an angle must be within ± 1 , the range of cosine of the steepness angle of toryx trailing string φ_2 is unlimited and is within $\pm \infty$.
- Unlike a general view that velocities can only be expressed by real numbers, translational velocity of the toryx trailing string V_{2t} can also be expressed by imaginary numbers. Consequently, the rotational velocity of the toryx trailing string V_{2r} can be either less or greater than ultimate string velocity c .

Based on the three toryx fundamental equations, one can readily derive the equations describing the spacetime properties of main toryx parameters. To make this task easier, we expressed the toryx spacetime parameters in relative terms in respect to the four constant parameters: inversion radius of trailing string r_i , circumference of the *inversion string* $2\pi r_i$, ultimate string velocity c , and the so-called *real string inversion frequency* f_i that is equal to:

$$f_i = \frac{c}{2\pi r_i} = \text{const.} \quad (13-4)$$

The obtained equations, shown in Table 13.2, allow us to analyze what happens with the toryx parameters as the relative radius of its leading string b_1 changes from $-\infty$ to $+\infty$. Since all the toryx parameters are expressed in relative terms, there is no need to know absolute values of any constants, including inversion radius of trailing string r_b , ultimate string velocity c , and real string inversion frequency f_i , to perform this analysis. In the process of this analysis we will witness some amazing metamorphoses of toryx shape.

INVERSION OF TORYX STRINGS

According to Equations (13-1) and (13-2b), the radius r_2 and steepness angle φ_2 of trailing string of the toryx change with the change of radius of its leading string r_1 . During this change the toryx undergoes through a dramatic transformation of its shape that involves inversion of its strings. We discussed the inversion phenomenon in Chapter 7. There is a great chance that you know the meaning of this word. You stumble upon inversion every time you turn your shirt inside out, sometimes by mistake. Some clothes designers even make use of the capability of clothes to be turned inside out and design them two-sided with different colors. The toryx strings can be turned inside out the same way.

To “visualize” the inversion states of the toryx strings, we presented the strings in the form of ribbons with their opposite surfaces colored in black and white. The inversion state of a string is directly related to the

sign of its radius. When the string radius is positive, the string is called *outverted*, and its color is assumed to be black. Conversely, when the radius is negative, the string is turned inside out; it is called *inverted*, and its color is white. Notably, in toryces, the outverted trailing strings are wound outside inversion string with radius r_i (Fig. 13.5), while in *antitoryces*, the trailing strings wound outside the inversion string are inverted.

For a quantitative description of the inversion state of the entire toryx, we use a so-called *toryx curvature factor* q that is equal to the ratio of radii of trailing and leading strings r_2 and r_1 with a negative sign:

$$q = -\frac{r_2}{r_1} = -\frac{b_1 - 1}{b_1} \quad (13-5)$$

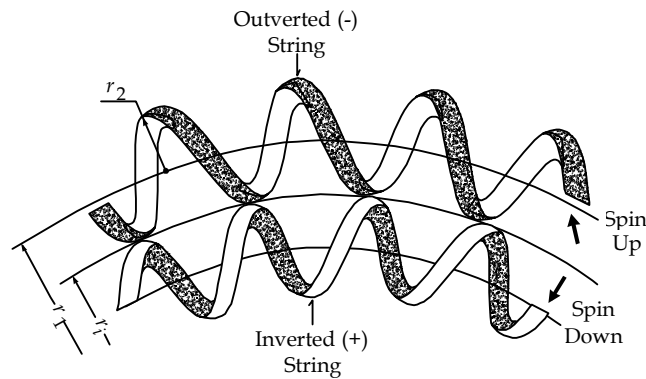


Fig. 13.5. Inversion of the toryx trailing string.

Let us consider a transformation of a trailing string wound outside inversion string (Fig. 13.5). Since in toryces this string is outverted, its radius is positive ($r_2 > 0$), and its external color is black. According to equations shown in Table 13.2, as long as r_1 stays greater than r_i , nothing out-of-ordinary happens when r_1 decreases: trailing string simply becomes slimmer, and the number of its windings w_2 decreases. But when $r_1 = r_i$, a real transformation of toryx occurs. Since in that case $r_2 = 0$, trailing string reduces to a circle with a single winding ($w_2 = 1$) that appears in Figure 13.5 as a colorless edge of a ribbon. When $r_1 < r_i$, the sign of its radius r_2 changes from positive to negative; trailing string turns inside out, or becomes inverted,. Consequently, its external color becomes white and its spin reverses. Importantly, the spin of the outverted trailing string can be either *up* (clockwise) or *down* (counter-

clockwise). The spin of the inverted trailing string will be respectively reversed to be either down or up.

Transformation of the toryx leading string proceeds in a similar manner (Fig. 13.6). When radius of leading string is positive ($r_1 > 0$), it is outverted, so its external color is black. When $r_1 = 0$, leading string reduces to a point, making a ribbon both dimensionless and colorless. When r_1 becomes negative ($r_1 < 0$), leading string turns inside out, or becomes inverted, making its external color white.

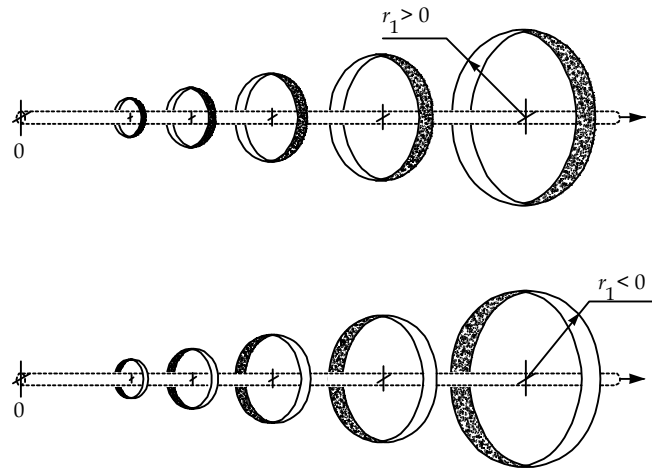


Fig. 13.6. Inversion of the toryx leading string.

VELOCITIES OF TORYX TRAILING STRING

We will use a very familiar to us Pythagorean Theorem for the right triangle to describe the relationships between velocities of trailing string. But, please do not be deceived by apparent simplicity of the Pythagorean equation, because we are going to expand its application into the range that is not conventionally used. Therefore, you may need to apply some of your imagination to visualize some unusual properties of toryx that make this element unique.

Consider a right triangle representing relative velocities of trailing string corresponding to the middle of the string: rotational velocity β_{2r} , translational velocity β_{2t} , and spiral velocity $\beta_2 = 1$. Then from the toryx fundamental spacetime equation (13-3) shown in Table 13.1 we obtain:

$$\beta_{2t}^2 + \beta_{2r}^2 = 1 \quad (13-6)$$

It is important to emphasize again that in the above equation the values of relative rotational velocity β_{2r} are not restricted, and can range from negative to positive infinity. Consequently, when $\beta_{2r} < 1$, β_{2r} is real, and when $\beta_{2r} > 1$, β_{2r} is imaginary. As shown in Table 13.2, relative rotational velocity β_{2r} is related to relative radius of leading string b_1 and string steepness angle φ_2 by the equation:

$$\beta_{2r} = \frac{b_1 - 1}{b_1} = \cos\varphi_2 \quad (13-7)$$

Thus, similar to the rotational velocity β_{2r} , the magnitude of $\cos\varphi_2$ can vary from negative to positive infinity.

Let us now consider the evolution of both rotational velocity β_{2r} and translational velocity β_{2t} with a change of steepness angle φ_2 of trailing string (Fig. 13.7).

Figure 13.7a - When $\varphi_2 = 0$ ($b_1 \rightarrow +\infty$), according to Equation (13-7), rotational velocity $\beta_{2r} = 1$, and the right triangle of velocities reduces to a straight line.

Figure 13.7b - Within the range $0 < \varphi_2 < 90^\circ$ ($1 < b_1 < +\infty$), the triangle of velocities contains both rotational β_{2r} and translational β_{2t} velocities, which magnitudes are expressed with real numbers. If β_{2r} is known, then β_{2t} can readily be calculated from Equation (13-6). For instance, for $\beta_{2r} = 0.99$, we obtain:

$$\beta_{2t} = \sqrt{1 - \beta_{2r}^2} = \sqrt{1 - 0.99^2} = 0.141$$

Figure 13.7c - When $\varphi_2 = 90^\circ$ ($b_1 = 1$), the triangle of velocities reduces again to a straight line when $\beta_{2t} = 1$ and $\beta_{2r} = 0$. This is a crossover point at which direction of rotational velocity β_{2r} changes.

Figure 13.7d - Within the range $90^\circ < \varphi_2 < 180^\circ$ ($1/2 < b_1 < 1$), the triangle of velocities contains both β_{2r} and β_{2t} but rotational velocity β_{2r} changes its sign, indicating that the trailing string is turned inside out.

Figure 13.7e - When $\varphi_2 = 180^\circ$ ($b_1 = 1/2$), the right triangle of velocities reduces to a straight line again. This is another crossover point at which $\beta_{2t} = 0$ and $\beta_{2r} = -1$. As long as the string steepness angle φ_2 does not exceed 180° , there is still nothing unusual in the behavior of the right triangle.

Figure 13.7f - Within the range $180^\circ < \varphi_2 < 270^\circ$ ($0 < b_1 < 1/2$), we encounter an interesting phenomenon: rotational velocity of trailing string exceeds ultimate string velocity, so $\beta_{2r} > 1$. Consequently, one side of the triangle of velocities becomes greater than its hypotenuse, and, as we described in Chapter 7, the triangle of velocities inverts. It

is easy to see that the triangle of velocities shown in Fig. 13.7f is inverted in respect to that shown in Fig. 13.7d. In the inverted triangle, rotational velocity β_{2r} becomes hypotenuse, and relative ultimate string velocity ($\beta_2 = 1$) converts into one of its legs.

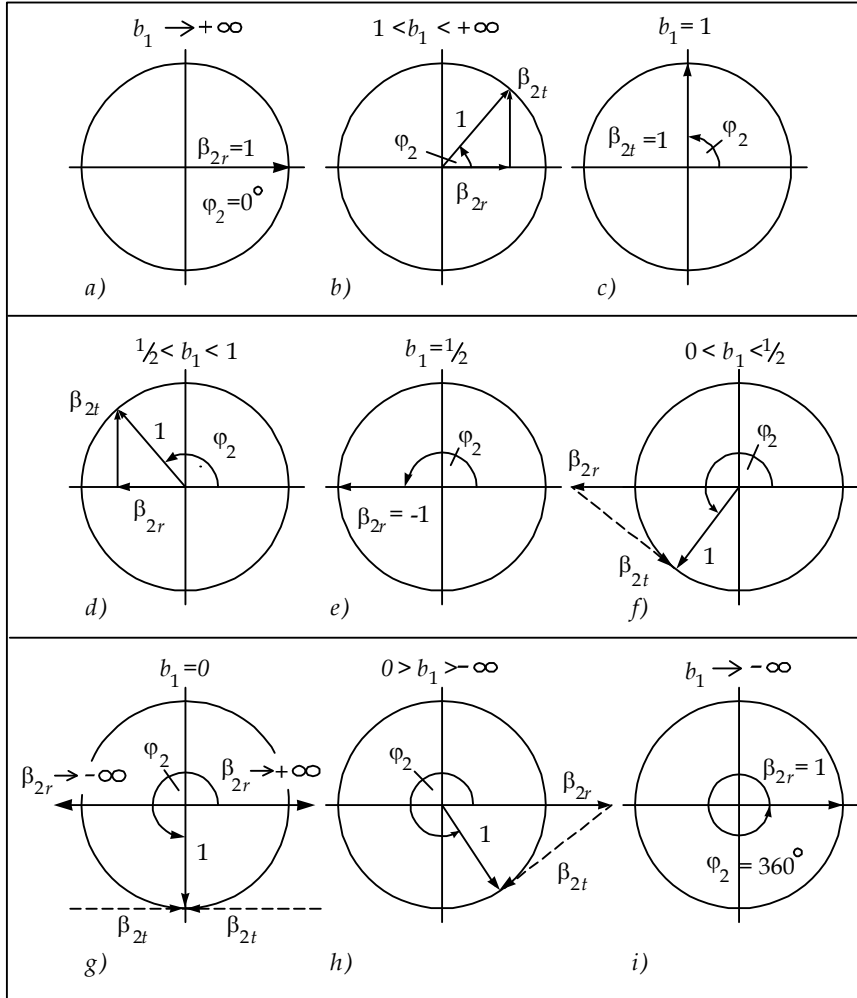


Fig. 13.7. Velocity hodographs of the toryx trailing string.

The inversion of the triangle of velocities does not prevent us from using the Pythagorean Theorem for calculation of translational velocity β_{2t} . For instance, for $\beta_{2r} = 1.01$, we will obtain from Equation (13-6) that translational velocity β_{2t} is expressed with an imaginary number:

$$\beta_{2t} = \sqrt{1 - \beta_{2r}^2} = \sqrt{1 - 1.01^2} = 0.141i$$

Thus, at $\varphi_2 = 180^\circ$, a transition takes place from a *real toryx* to an *imaginary toryx*. It is useful to remember that in the real toryx, the rotational velocity of trailing string V_{2r} is less than ultimate string velocity ($\beta_{2r} < 1$), while in the imaginary toryx, it is greater than ultimate string velocity ($\beta_{2r} > 1$). As φ_2 continues to increase, b_1 gets closer to zero, negative value of β_{2r} increases, and the right triangle of velocities continues to elongate.

Figure 13.7g – At $\varphi_2 = 270^\circ$ ($b_1 = 0$), we pass through another crossover point at which the direction of rotational velocity β_{2r} reverses from negative infinity to positive infinity.

Figure 13.7h – Within the range $270^\circ < \varphi_2 < 360^\circ$ ($0 > b_1 > -\infty$), as φ_2 continues to increase, negative value of b_1 increases, positive value of β_{2r} decreases, and the right triangle of velocities becomes smaller.

Figure 13.7i – When $\varphi_2 = 360^\circ$ ($b_1 \rightarrow -\infty$), the right triangle of velocities reduces to a straight line, and rotational velocity β_{2r} becomes equal to 1. Now, compare Figures 13.7a and 13.7i. They are completely identical in all aspects, except for one important difference. In Figure 13.7a, b_1 approaches positive infinity ($+\infty$), while in Figure 13.7i it approaches negative infinity ($-\infty$). Here you are witnessing a great *phenomenon of merging positive and negative infinities*. This phenomenon, however, is not limited to the relative radii of leading string b_1 . The infinities also merge for several other toryx parameters when $\varphi_2 = 270^\circ$ ($b_1 = 0$). As we described in Chapter 7, about a century and a half ago Georg Riemann produced an ingenious mathematical example of merging positive and negative infinities. Riemann employed projective geometry to achieve his goal. This phenomenon reveals itself in toryx without using any additional techniques.

So far, we have described the behavior of the middle translational and rotational velocities corresponding to the middle of the trailing string. We will now consider the dynamics of translational and rotational velocities as the trailing string makes one cycle along its spiral path. It is clear from Figure 13.8 that translational velocity β_{2t} at each point of the trailing string is proportional to the distance from the toryx center. At the same time, rotational velocity β_{2r} of the trailing string changes in such a way that each point of the trailing string propagates at a constant spiral string velocity equal to the ultimate string velocity. Thus, β_{2r} can be determined at each point from Equation (13-6).

Table 13.3 shows the equations for relative peripheral translational velocities (β'_{2t} and β''_{2t}) and relative peripheral rotational velocities (β'_{2r} and β''_{2r}) of trailing string. From these equations we find that for some real toryces, the peripheral translational velocity of trailing string becomes superluminal, while its middle translational velocity remains

subluminal. This occurs when relative radius of leading string is within the range:

$$0.5437 < b_1 < 6.2223 \tag{13-8}$$

Table 13.3. Relative peripheral and middle velocities of trailing string.

Points on trailing string (Fig. 13.8)		
Inner point a'	Middle point a	Outer point a''
$\beta'_{2t} = \frac{\sqrt{2b_1 - 1}}{b_1^2}$	$\beta_{2t} = \frac{\sqrt{2b_1 - 1}}{b_1}$	$\beta''_{2t} = \frac{(2b_1 - 1)\sqrt{2b_1 - 1}}{b_1^2}$
$\beta'_{2r} = \frac{\sqrt{b_1^4 - 2b_1 + 1}}{b_1^2}$	$\beta_{2r} = \frac{b_1 - 1}{b_1}$	$\beta''_{2r} = \frac{\sqrt{b_1^4 - (2b_1 - 1)^3}}{b_1^2}$

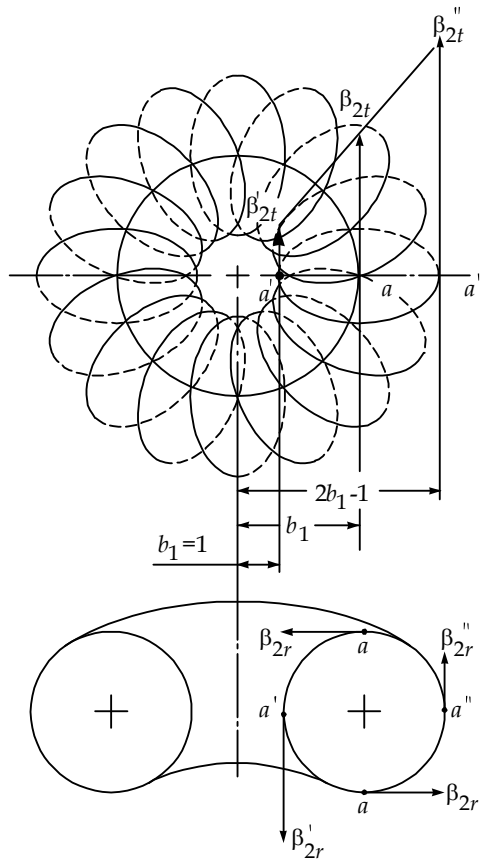


Fig. 13.8. Peripheral and middle velocities of toryx trailing string.

METAMORPHOSES OF THE TORYX SHAPE

We will use now the equations for the spacetime properties of toryx shown in Table 13.2 to visualize fantastic spacetime transformations of the toryx shape. Figure 13.9 illustrates ten different appearances of toryx as the steepness angle of trailing string φ_2 changes from 0^0 to 360^0 . These appearances correspond to the change of relative radius of leading string b_1 from positive infinity ($+\infty$) to negative infinity ($-\infty$).

Shown in each view with dotted lines are the circles with the same relative radius $b_1 = 1$. Each circle represents the inversion string. We used two criteria for classification of toryces. The first criterion is the reality of rotational velocity of the toryx leading string V_{1r} that can be either *real* or *imaginary*. The second criterion is the sign of the toryx curvature factor q that can be either *positive* or *negative*. Consequently, the toryces are divided into four principle groups:

1. Real negative toryces
2. Real positive toryces
3. Imaginary positive toryces
4. Imaginary negative toryces.

Real negative toryces ($0^0 \leq \varphi_2 \leq 90^0$) and ($1 \leq b_1 < +\infty$) – When $\varphi_2 = 0^0$ and $b_1 \rightarrow +\infty$, relative radius of the toryx trailing string b_2 approaches positive infinity ($b_2 \rightarrow +\infty$). Therefore, trailing string appears as an infinitely long straight line tangential to the inversion string called the *negative inversion string*. This toryx has the infinite number of windings w_2 ; its trailing string propagates at rotational velocity equal to the ultimate string velocity c ($\beta_{2r} = 1$), while its translational velocity is equal to zero ($\beta_{2t} = 0$). Also equal to zero are frequencies of both leading and trailing strings ($\delta_1 = \delta_2 = 0$).

As φ_2 increases and b_1 decreases, relative radius of the toryx trailing string b_2 decreases accordingly, making the trailing string to look like a toroidal spiral. At the end of the range, when $\varphi_2 = 90^0$ and $b_1 = 1$, the trailing string disappears and the toryx reduces to a circle called the *real inversion string*.

Real positive toryces ($90^0 \leq \varphi_2 \leq 180^0$) and ($1/2 \leq b_1 \leq 1$) – Within this range, toryx is still real, but its trailing string becomes inverted, and windings are now located inside the inversion string. Consequently, the direction of rotational velocity of trailing string reverses ($\beta_{2r} < 0$). As b_1 becomes less than 1, the number of windings w_2 and absolute value of β_{2r} increase, while translational velocity β_{2t} decreases. Frequencies of both leading and trailing strings become greater than the string base frequency ($\delta_1 > 1$; $\delta_2 > 1$).

At the end of the range, when $\varphi_2 = 180^\circ$ and $b_1 = \frac{1}{2}$, toryx reduces to a circle with radius equal to one half of inversion radius r_i . It is called the *positive inversion string*. In this toryx the number of windings w_2 approaches infinity. Its trailing string propagates at rotational velocity equal to the negative ultimate string velocity $-c$ ($\beta_{2r} = -1$), while its translational velocity is equal to zero ($\beta_{2t} = 0$). Also equal to zero is frequency of leading string ($\delta_1 = 0$), while frequency of trailing string becomes two times greater than the string base frequency ($\delta_2 = 2$).

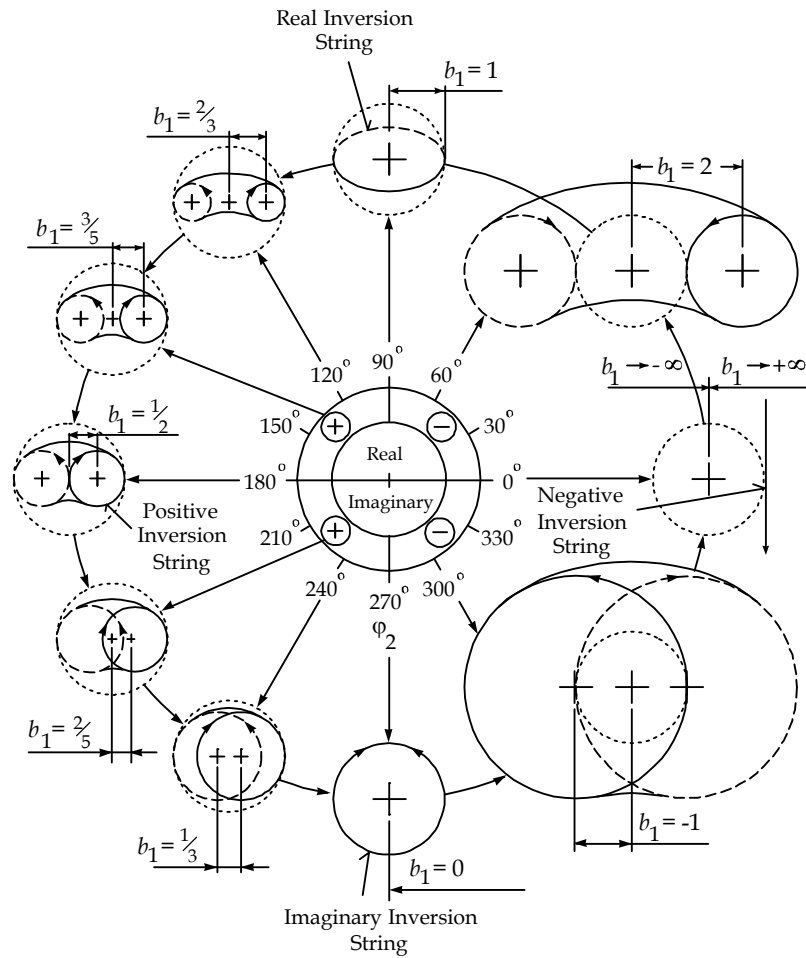


Figure 13.9. Cross-sectional views of toryces.

Imaginary positive toryces ($180^\circ \leq \varphi_2 \leq 270^\circ$) and ($0 \leq b_1 \leq \frac{1}{2}$) – Within this range, windings of trailing string overlap each other in toryx eye like in a so-called *spindle torus*. Its trailing string remains inverted and its windings stay inside inversion string. Therefore, rotational

velocity of trailing string remains negative ($\beta_{2r} < 0$) and is expressed with a real number. Also expressed with a real number is the frequency of trailing string δ_2 . Several parameters, including w_2 , β_{2s} , and δ_1 , are expressed with imaginary numbers. Within this range, relative rotational velocity β_{2r} and relative frequency δ_2 increase with decrease of b_1 .

At the very end of the range, when $\varphi_2 \rightarrow 270^0$ and $b_1 \rightarrow 0$, toryx reduces to a circle with radius r_i called the *imaginary inversion string*. It is located in the plane perpendicular to the plane of the real inversion string. In this toryx, the number of windings w_2 is equal to zero ($w_2 = 0$), both parameters of trailing string, β_{2r} and δ_2 , approach negative infinity, while the two other toryx parameters, β_{2s} and δ_1 , approach imaginary positive infinity.

Imaginary negative toryces ($270^0 \leq \varphi_2 \leq 360^0$) and ($-\infty < b_1 \leq 0$) - At the very beginning of the range, toryx appears as the *imaginary inversion string* that is the same as the imaginary inversion string for the imaginary positive toryces, except that the values of β_{2r} , δ_2 , β_{2s} and δ_1 change their signs. Within this range, the windings of trailing string also overlap each other, but in a different manner than in the imaginary positive toryx. In this toryx, trailing string becomes outverted, and its windings are now wrapped outside the inversion trailing string. Rotational velocity of trailing string becomes positive ($\beta_{2r} > 0$), and it is still expressed with real numbers. Also expressed with real numbers is the frequency of trailing string δ_2 . Both β_{2r} and δ_2 decrease as the absolute value of b_1 increases. Within this range, several parameters, including w_2 , β_{2s} , and δ_1 , are expressed with imaginary numbers.

At the end of the range, when $\varphi_2 = 360^0$ and $b_1 \rightarrow -\infty$, toryx reduces to the same *negative inversion string* ($\varphi_2 = 0^0$ and $b_1 \rightarrow +\infty$) that makes the real negative toryx. As we discussed earlier, positive and negative infinite values of b_1 merge at this point. As in the negative inversion string of the real negative toryx, this string has the infinite imaginary number of windings w_2 ; it propagates at rotational velocity equal to the ultimate string velocity c ($\beta_{2r} = 1$), while its translational velocity is equal to zero ($\beta_{2s} = 0$). Also equal to zero are frequencies of both leading and trailing strings ($\delta_1 = \delta_2 = 0$).

CONSTRUCTION OF HELYX

Similarly to the toryx, the helyx is a double-level helicola. In the helyx, the first level of helicola is made of one double-helical spiral (Fig. 13.10). There is an easy way to visualize the double-helical spiral. There is an easy way to visualize the double-helical spiral. Consider two points, a and b , rotating around a pivot point m with rotational velocity \vec{V}_{1r} , while the pivot point m propagates along a straight line O_1O_1

with translational velocity \tilde{V}_{1t} . Each point, a and b , leaves a helical spiral trace A_1 winding around the straight line O_1O_1 . The two traces A_1 are separated from one another by 180 degrees and form a double helix called the *helyx leading string*.

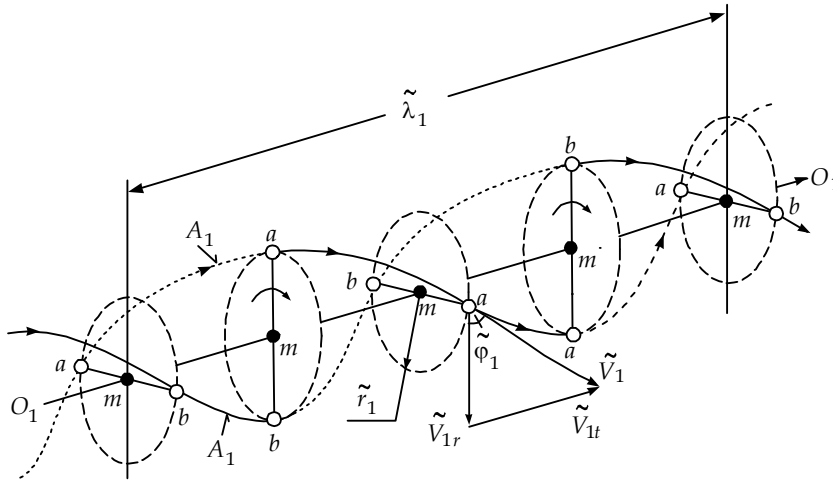


Figure 13.10. Leading string of helyx.

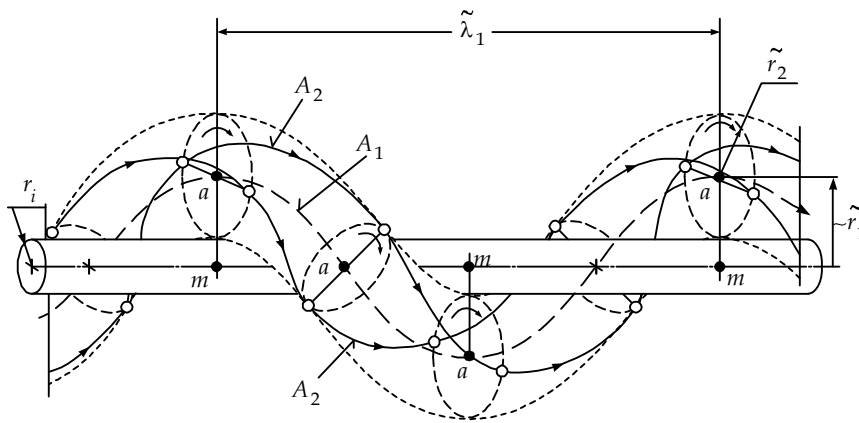


Figure 13.11. Construction of one of two double-helical leading strings.

The second level of the helyx is made of two double helices, each wrapped around one of the helical spirals of leading string. The two double helices of the second level of the helyx form the *helyx trailing string*. For the sake of simplicity, Figure 13.11 shows a helyx with only

one double-helical spiral of leading string. There the leading string is represented by a helical trace A_1 that is accompanied by two helical traces A_2 representing the trailing string.

In spite of many features common for both the helyx and the toryx, the helyx is different than the toryx in several ways. First of all, unlike the double-circular leading string of the toryx, the leading string of the helyx is double-helical. Secondly, the steepness angle of the helyx trailing strings $\tilde{\varphi}_2$ is much greater than the steepness angle φ_2 of the toryx. Also different are the magnitudes and realities of rotational and translational velocities of the trailing strings. In the toryx, rotational velocity of trailing string is always real; it can vary from negative to positive infinity, while translational velocity can be either real or imaginary. In the helyx, translational velocity of trailing string is always real and can vary from negative to positive infinity, while rotational velocity can be either real or imaginary.

SPACETIME PARAMETERS OF HELYX

In the diagrams shown in Figure 13.12 the spacetime parameters of leading and trailing strings form the sides of right triangles. Therefore, we can readily establish the relationships between these parameters by using the Pythagorean Theorem.

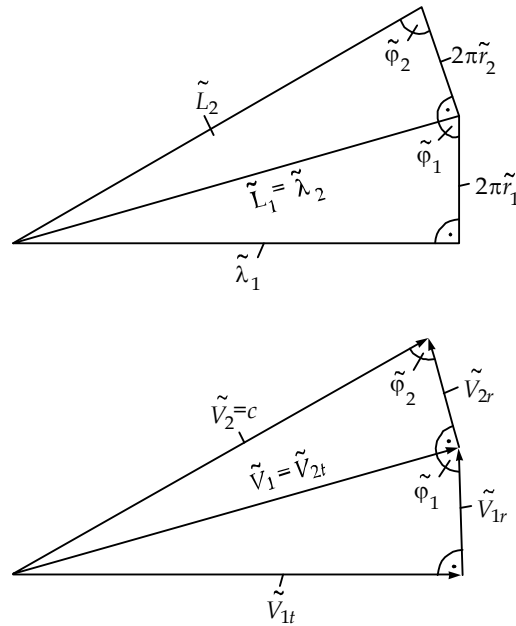


Figure 13.12. Spacetime parameters of helyx.

Helical trailing strings of the helyx propagate along their helical paths in synchrony with helical leading strings. Consequently, spiral velocity of leading string \tilde{V}_1 is equal to translational velocity of trailing string \tilde{V}_{2t} ($\tilde{V}_1 = \tilde{V}_{2t}$). Table 13.4 allows us to compare the relationships between string velocities in helyx and toryx. Similarly to the toryx, the spacetime properties of the helyx are governed by four fundamental equations shown in Table 13.5.

Table 13.4. Relationships between string velocities in helyx and toryx.

Helyx		Toryx	
Leading string	Trailing string	Leading string	Trailing string
$\tilde{V}_{1t} \neq 0$	$\tilde{V}_{2t} \neq 0$	$V_{1t} = 0$	$V_{2t} \neq 0$
$\tilde{V}_1^2 = \tilde{V}_{1t}^2 + \tilde{V}_{1r}^2$	$\tilde{V}_2^2 = \tilde{V}_{2t}^2 + \tilde{V}_{2r}^2$	$V_1^2 = V_{1t}^2 + V_{1r}^2$	$V_2^2 = V_{2t}^2 + V_{2r}^2$
$\tilde{V}_{2t} = \tilde{V}_1$		$V_{2t} = V_{1r} = V_1$	
$\tilde{V}_2^2 = \tilde{V}_{1t}^2 + \tilde{V}_{1r}^2 + \tilde{V}_{2r}^2$		$V_2^2 = V_{1r}^2 + V_{2r}^2$	

One can clearly see some similarity between the fundamental spacetime equations for helyx (Table 13.5) and toryx (Table 13.1). Equations for inversion radius of trailing string r_i are identical. For the helyx, the ratio of radii of trailing and leading strings \tilde{r}_2 and \tilde{r}_1 is equal to the *sine* of steepness angle, rather than to the *cosine* of this angle used for toryx. Similarly to the toryx, spiral velocity of the helyx trailing string \tilde{V}_2 is equal to the ultimate string velocity c . Adding to the similarities between helyx and toryx is the fact that for both of them the inversion radius of trailing string r_i and the real string inversion frequency f_i are respectively expressed by the same equations.

Table 13.5. Fundamental spacetime equations for helyx.

Parameter	Equation	Range
Inversion radius of trailing string	$r_i = \tilde{r}_1 - \tilde{r}_2 = const. \quad (13-9)$	$-\infty < \tilde{r}_1 < +\infty$ $-\infty < \tilde{r}_2 < +\infty$
Length of one winding of trailing string	$\tilde{\lambda}_2 = \tilde{L}_1 \quad (13-10)$	$-\infty < \tilde{L}_1 < +\infty$
Steepness angle of trailing string	$\sin \tilde{\varphi}_2 = \frac{\tilde{r}_2}{\tilde{r}_1} \quad (13-11)$	$-\infty < \sin \tilde{\varphi}_2 < +\infty$
Spiral velocity of trailing string.	$\tilde{V}_2 = \sqrt{\tilde{V}_{1t}^2 + \tilde{V}_{1r}^2 + \tilde{V}_{2r}^2} = c \quad (13-12)$	$-\infty < \tilde{V}_{1t}^2 < +\infty$ $-\infty < \tilde{V}_{1r}^2 < +\infty$

As we have done in application to the toryx, we can take advantage of constancy of inversion radius r_i , ultimate string velocity c , and real inversion string frequency f_i to express spacetime parameters of helyx in relative terms. This will make these parameters dimensionless, drastically simplifying mathematical model. With these simplifications, we can readily derive equations for the helyx spacetime parameters as a function of relative radii of their leading string \tilde{b}_1 (see Table 13.6).

Table 13.6. Spacetime properties of the helyx leading and trailing strings.

Parameters	Leading string	Trailing string
Relative string radius	$\tilde{b}_1 = \frac{\tilde{r}_1}{r_i}$	$\tilde{b}_2 = \frac{\tilde{r}_2}{r_i} = \tilde{b}_1 - 1$
Steepness angle	$\cos \tilde{\varphi}_1 = \frac{\tilde{b}_1 \sqrt{2\tilde{b}_1 - 1}}{(\tilde{b}_1 - 1)^2}$	$\sin \tilde{\varphi}_2 = \frac{\tilde{b}_1 - 1}{\tilde{b}_1}$
Relative wavelength	$\tilde{\eta}_1 = \frac{\tilde{\lambda}_1}{2\pi r_i} = \sqrt{\frac{(\tilde{b}_1 - 1)^4 - \tilde{b}_1^2 (2\tilde{b}_1 - 1)}{2\tilde{b}_1 - 1}}$	$\tilde{\eta}_2 = \frac{\tilde{\lambda}_2}{2\pi r_i} = \frac{(\tilde{b}_1 - 1)^2}{\sqrt{2\tilde{b}_1 - 1}}$
Relative length of one winding	$\tilde{l}_1 = \frac{\tilde{L}_1}{2\pi r_i} = \frac{(\tilde{b}_1 - 1)^2}{\sqrt{2\tilde{b}_1 - 1}}$	$\tilde{l}_2 = \frac{\tilde{L}_2}{2\pi r_i} = \frac{\tilde{b}_1 (\tilde{b}_1 - 1)}{\sqrt{2\tilde{b}_1 - 1}}$
Number of windings per string	$\tilde{w}_1 = 1$	$\tilde{w}_2 = 1$
Relative translational velocity	$\tilde{\beta}_{1t} = \frac{\tilde{V}_{1t}}{c} = \frac{\sqrt{(\tilde{b}_1 - 1)^4 - \tilde{b}_1^2 (2\tilde{b}_1 - 1)}}{\tilde{b}_1 (\tilde{b}_1 - 1)}$	$\tilde{\beta}_{2t} = \frac{\tilde{V}_{2t}}{c} = \frac{\tilde{b}_1 - 1}{\tilde{b}_1}$
Relative rotational velocity	$\tilde{\beta}_{1r} = \frac{\tilde{V}_{1r}}{c} = \frac{\sqrt{2\tilde{b}_1 - 1}}{\tilde{b}_1 - 1}$	$\tilde{\beta}_{2r} = \frac{\tilde{V}_{2r}}{c} = \frac{\sqrt{2\tilde{b}_1 - 1}}{\tilde{b}_1}$
Relative spiral velocity	$\tilde{\beta}_1 = \frac{\tilde{V}_1}{c} = \frac{\tilde{b}_1 - 1}{\tilde{b}_1}$	$\tilde{\beta}_2 = \frac{\tilde{V}_2}{c} = 1$
Relative frequency	$\tilde{\delta}_1 = \frac{\tilde{f}_1}{f_i} = \frac{\sqrt{2\tilde{b}_1 - 1}}{\tilde{b}_1 (\tilde{b}_1 - 1)}$	$\tilde{\delta}_2 = \frac{\tilde{f}_2}{f_i} = \frac{\sqrt{2\tilde{b}_1 - 1}}{\tilde{b}_1 (\tilde{b}_1 - 1)}$
Relative time period	$\tilde{t}_1 = \tilde{T}_1 f_i = \frac{\tilde{b}_1 (\tilde{b}_1 - 1)}{\sqrt{2\tilde{b}_1 - 1}}$	$\tilde{t}_2 = \tilde{T}_2 f_i = \frac{\tilde{b}_1 (\tilde{b}_1 - 1)}{\sqrt{2\tilde{b}_1 - 1}}$

The helyx curvature factor \tilde{q} is equal to:

$$\tilde{q} = -\sqrt{1 - \left(\frac{\tilde{r}_2}{\tilde{r}_1}\right)^2} = -\frac{\sqrt{2\tilde{b}_1 - 1}}{\tilde{b}_1} \quad (13-13)$$

Proposed fundamental spacetime equations for both toryx and helyx significantly reduced possible spacetime configurations of these elements. At the same time, they provided these elements with unique transformations of their shapes that include the changes of their reality, inversion of their strings, toryx curvature factor, and spin. Table 13.7 summarizes the spacetime transformation states of toryces and helycles. In *antitoryx* and *antihelyx*, trailing strings are turned inside out in respect to their states in toryx and helyx (see Table 13.8). The black and white colors of the toryx strings shown in Tables 13.7 and 13.8 correspond to the colors depicted in Figures 13.5 and 13.6.

Table 13.7. Spacetime transformation states of toryces and helycles.

Parameter	Ranges of b_1 and \tilde{b}_1			
	$-\infty \leftrightarrow 0$	$0 \leftrightarrow 0.5$	$0.5 \leftrightarrow 1.0$	$1.0 \leftrightarrow +\infty$
Reality	Imaginary	Imaginary	Real	Real
Inversion state of leading string	White $r_1 < 0$	Black $r_1 > 0$	Black $r_1 > 0$	Black $r_1 > 0$
Inversion state of trailing string	White $r_2 < 0$	White $r_2 < 0$	White $r_2 < 0$	Black $r_2 > 0$
Sign of curvature factor q	(-)	(+)	(+)	(-)
Spin of trailing string	Up (down)	Down (up)	Down (up)	Up (down)

Table 13.8. Spacetime transformation states of antitoryces and antihelyces.

Parameter	Ranges of b_1 and \tilde{b}_1			
	$-\infty \leftrightarrow 0$	$0 \leftrightarrow 0.5$	$0.5 \leftrightarrow 1.0$	$1.0 \leftrightarrow +\infty$
Reality	Imaginary	Imaginary	Real	Real
Inversion state of leading string	White $r_1 < 0$	Black $r_1 > 0$	Black $r_1 > 0$	Black $r_1 > 0$
Inversion state of trailing string	Black $r_2 > 0$	Black $r_2 > 0$	Black $r_2 > 0$	White $r_2 < 0$
Sign of curvature factor q	(+)	(-)	(-)	(+)
Spin of trailing string	Up (down)	Down (up)	Down (up)	Up (down)

